

AD-A056 425

BALLISTIC RESEARCH LABS ABERDEEN PROVING GROUND MD
LASER-INDUCED OPTO-ACOUSTIC PULSES IN A FLAME, (U)
JUN 78 D R CROSLLEY

F/G 21/2

UNCLASSIFIED

NL

| OF |

AD
A056425



END
DATE
FILMED
8-78
DDC

AD A056425

CROSLEY

LEVEL II



12 15 p.

6

LASER-INDUCED OPTO-ACOUSTIC PULSES IN A FLAME,

JUN 1978

10

11

DAVID R. CROSLEY, DR.
 BALLISTIC RESEARCH LABORATORY
 ABERDEEN PROVING GROUND, MD 21005

DDC
 RECORDED
 JUL 10 1978
 D

INTRODUCTION

Laser Probes and Combustion Chemistry

The application of lasers to the study of combustion processes offers a wealth of information of diverse kinds. Many of these new techniques - in particular laser-excited fluorescence, ordinary Raman scattering, and coherent anti-stokes Raman spectroscopy - are aimed at the measurement of concentrations of individual molecular species at partial pressures ranging from several atmospheres down to 10^{-10} torr. (1) The use of scanning lasers permits one to map out energy level population distributions within ground electronic states, with an ease and accuracy previously possible only for excited states. From such information can be obtained temperatures corresponding to different degrees of freedom. Measurement of laser absorption line-shapes within flames provides data on energy transfer rates and translational temperatures. The recent successful observation of two-photon excitation of Na in a 1-atm pressure flame (2) suggests numerous possibilities for probing those species now inaccessible by present-day commercial available lasers with one-photon excitation.

The use of the full arsenal of these laser techniques so far demonstrated would provide a nearly complete experimental characterization of a process undergoing combustion. Of course, the use of lasers means, almost necessarily, a high degree of spatial resolution: focusing to 100 μ beam diameter is generally easy. Pulsed lasers of various types yield concomitant temporal resolution down to several nsec. Consequently spatial profiles, over time periods unblurred by turbulence, can be obtained for these quantities of interest. It

78 06 12 048

DISTRIBUTION STATEMENT A

Approved for public release;
 Distribution Unlimited

.050 750

mt

AU NO.

DDC FILE COPY

CROSLEY

should be noted that, in addition, laser probes are non-perturbative. That is, they introduce no physical barriers into the gas flow or provide surfaces which could cause heterogeneous catalysis influencing the chemistry. Although the presence of particulate matter can be a serious problem, extremes of temperature and pressure offer no hostility to the laser beam itself.

The field likely to benefit most from this detailed picture is that of combustion chemistry. The information on transient, reactive species will provide the key to the mechanistic chemical kinetics heretofore usually only inferred from the composition of final products. Data on state distributions will directly address the questions of disequilibrium in combustion systems, widely recognized as existing but seldom accounted for in mechanistic schemes. In fact, this combination of experimental probes using laser-based techniques together with theoretical chemical kinetic modelling on modern large computers has been heralded(3) as promising - finally - significant advancement in the enormously complex problem of the chemistry of combustion. An understanding of the chemistry pertinent to ballistic systems will undoubtedly require such models tied in detail to copious laser-based experiments (as well as measurements with other techniques) under controlled laboratory conditions and proven by agreement with the necessarily more limited data available on real systems.

Nearly all of the currently available laser probe methods rely on the scattering or emission of light as the mode of detection. While this can be a highly sensitive method under many conditions, there are other situations in which it is less suitable. For example, high excited state quenching rates reduce the degree of emitted fluorescence, and Raman-scattered photons could be absorbed by some interfering molecular species. One recent alternative method is the optogalvanic effect,(4) in which the yield of collisionally produced ions is enhanced by promotion, using laser excitation, to excited electronic states lying nearer to the ionization continuum than does the ground state.

Opto-Acoustic Pulses

We discuss here another means of detection of the absorption of laser radiation by individual species in a flame environment; the production of opto-acoustic pulses in a flame at 1-atm pressure.(5) The flame is seeded with alkali atoms and a pulsed laser is tuned to the appropriate absorption line. While some of the electronically excited atoms fluoresce, the vast majority lose their energy by collision with other gases present in the flame. This energy ultimately *→ next page*

SECTION 10	White Section	<input checked="" type="checkbox"/>	<input type="checkbox"/>
11	Left Section	<input type="checkbox"/>	<input type="checkbox"/>
12	Right Section	<input type="checkbox"/>	<input type="checkbox"/>
13	Bottom Section	<input type="checkbox"/>	<input type="checkbox"/>
14	Top Section	<input type="checkbox"/>	<input type="checkbox"/>
15	Center Section	<input type="checkbox"/>	<input type="checkbox"/>
16	Left Section	<input type="checkbox"/>	<input type="checkbox"/>
17	Right Section	<input type="checkbox"/>	<input type="checkbox"/>
18	Bottom Section	<input type="checkbox"/>	<input type="checkbox"/>
19	Top Section	<input type="checkbox"/>	<input type="checkbox"/>
20	Center Section	<input type="checkbox"/>	<input type="checkbox"/>
21	Left Section	<input type="checkbox"/>	<input type="checkbox"/>
22	Right Section	<input type="checkbox"/>	<input type="checkbox"/>
23	Bottom Section	<input type="checkbox"/>	<input type="checkbox"/>
24	Top Section	<input type="checkbox"/>	<input type="checkbox"/>
25	Center Section	<input type="checkbox"/>	<input type="checkbox"/>
26	Left Section	<input type="checkbox"/>	<input type="checkbox"/>
27	Right Section	<input type="checkbox"/>	<input type="checkbox"/>
28	Bottom Section	<input type="checkbox"/>	<input type="checkbox"/>
29	Top Section	<input type="checkbox"/>	<input type="checkbox"/>
30	Center Section	<input type="checkbox"/>	<input type="checkbox"/>
31	Left Section	<input type="checkbox"/>	<input type="checkbox"/>
32	Right Section	<input type="checkbox"/>	<input type="checkbox"/>
33	Bottom Section	<input type="checkbox"/>	<input type="checkbox"/>
34	Top Section	<input type="checkbox"/>	<input type="checkbox"/>
35	Center Section	<input type="checkbox"/>	<input type="checkbox"/>
36	Left Section	<input type="checkbox"/>	<input type="checkbox"/>
37	Right Section	<input type="checkbox"/>	<input type="checkbox"/>
38	Bottom Section	<input type="checkbox"/>	<input type="checkbox"/>
39	Top Section	<input type="checkbox"/>	<input type="checkbox"/>
40	Center Section	<input type="checkbox"/>	<input type="checkbox"/>
41	Left Section	<input type="checkbox"/>	<input type="checkbox"/>
42	Right Section	<input type="checkbox"/>	<input type="checkbox"/>
43	Bottom Section	<input type="checkbox"/>	<input type="checkbox"/>
44	Top Section	<input type="checkbox"/>	<input type="checkbox"/>
45	Center Section	<input type="checkbox"/>	<input type="checkbox"/>
46	Left Section	<input type="checkbox"/>	<input type="checkbox"/>
47	Right Section	<input type="checkbox"/>	<input type="checkbox"/>
48	Bottom Section	<input type="checkbox"/>	<input type="checkbox"/>
49	Top Section	<input type="checkbox"/>	<input type="checkbox"/>
50	Center Section	<input type="checkbox"/>	<input type="checkbox"/>
51	Left Section	<input type="checkbox"/>	<input type="checkbox"/>
52	Right Section	<input type="checkbox"/>	<input type="checkbox"/>
53	Bottom Section	<input type="checkbox"/>	<input type="checkbox"/>
54	Top Section	<input type="checkbox"/>	<input type="checkbox"/>
55	Center Section	<input type="checkbox"/>	<input type="checkbox"/>
56	Left Section	<input type="checkbox"/>	<input type="checkbox"/>
57	Right Section	<input type="checkbox"/>	<input type="checkbox"/>
58	Bottom Section	<input type="checkbox"/>	<input type="checkbox"/>
59	Top Section	<input type="checkbox"/>	<input type="checkbox"/>
60	Center Section	<input type="checkbox"/>	<input type="checkbox"/>
61	Left Section	<input type="checkbox"/>	<input type="checkbox"/>
62	Right Section	<input type="checkbox"/>	<input type="checkbox"/>
63	Bottom Section	<input type="checkbox"/>	<input type="checkbox"/>
64	Top Section	<input type="checkbox"/>	<input type="checkbox"/>
65	Center Section	<input type="checkbox"/>	<input type="checkbox"/>
66	Left Section	<input type="checkbox"/>	<input type="checkbox"/>
67	Right Section	<input type="checkbox"/>	<input type="checkbox"/>
68	Bottom Section	<input type="checkbox"/>	<input type="checkbox"/>
69	Top Section	<input type="checkbox"/>	<input type="checkbox"/>
70	Center Section	<input type="checkbox"/>	<input type="checkbox"/>
71	Left Section	<input type="checkbox"/>	<input type="checkbox"/>
72	Right Section	<input type="checkbox"/>	<input type="checkbox"/>
73	Bottom Section	<input type="checkbox"/>	<input type="checkbox"/>
74	Top Section	<input type="checkbox"/>	<input type="checkbox"/>
75	Center Section	<input type="checkbox"/>	<input type="checkbox"/>
76	Left Section	<input type="checkbox"/>	<input type="checkbox"/>
77	Right Section	<input type="checkbox"/>	<input type="checkbox"/>
78	Bottom Section	<input type="checkbox"/>	<input type="checkbox"/>
79	Top Section	<input type="checkbox"/>	<input type="checkbox"/>
80	Center Section	<input type="checkbox"/>	<input type="checkbox"/>
81	Left Section	<input type="checkbox"/>	<input type="checkbox"/>
82	Right Section	<input type="checkbox"/>	<input type="checkbox"/>
83	Bottom Section	<input type="checkbox"/>	<input type="checkbox"/>
84	Top Section	<input type="checkbox"/>	<input type="checkbox"/>
85	Center Section	<input type="checkbox"/>	<input type="checkbox"/>
86	Left Section	<input type="checkbox"/>	<input type="checkbox"/>
87	Right Section	<input type="checkbox"/>	<input type="checkbox"/>
88	Bottom Section	<input type="checkbox"/>	<input type="checkbox"/>
89	Top Section	<input type="checkbox"/>	<input type="checkbox"/>
90	Center Section	<input type="checkbox"/>	<input type="checkbox"/>
91	Left Section	<input type="checkbox"/>	<input type="checkbox"/>
92	Right Section	<input type="checkbox"/>	<input type="checkbox"/>
93	Bottom Section	<input type="checkbox"/>	<input type="checkbox"/>
94	Top Section	<input type="checkbox"/>	<input type="checkbox"/>
95	Center Section	<input type="checkbox"/>	<input type="checkbox"/>
96	Left Section	<input type="checkbox"/>	<input type="checkbox"/>
97	Right Section	<input type="checkbox"/>	<input type="checkbox"/>
98	Bottom Section	<input type="checkbox"/>	<input type="checkbox"/>
99	Top Section	<input type="checkbox"/>	<input type="checkbox"/>
100	Center Section	<input type="checkbox"/>	<input type="checkbox"/>

78 06 12 048

CROSLEY

(though rapidly) is converted into translational kinetic energy of the flame gases, producing a pulsed pressure wave which expands from the region illuminated by the laser. This sound wave is readily audible to an observer in the vicinity of the burner.* Quantitative measurements are made using a microphone, and show that the technique is very sensitive and accurate, and perturbs neither the gas dynamics nor chemical kinetics of the flame.

Now the opto-acoustic effect in general, *viz.*, the conversion of optical to acoustical energy through absorption and collisional quenching, has long been known as a means of sensitively detecting the absorption of radiation. What is here newly demonstrated is the nature of its occurrence following pulsed excitation, and the existence of the effect under *in situ* conditions on a 1-atm pressure flame burner (in contrast to the typical mode of operation using specially constructed cells at low pressure).

In addition to exploiting its detection capabilities, we have also utilized the effect to perform measurements of the speed of sound within the flame on a spatially resolved basis. These data provide information on the translational motion of the flame gases. This aspect may prove especially useful for environments too hostile to insert thermocouple probes or processes too rapid to obtain usable thermocouple response.

Finally, we note that the form of the pressure wave appears to contain information concerning density gradients within the flame, and may be influenced by bulk energy transfer within the flame gases. However, we have not pursued these possibilities in a quantitative manner in this study.

* In fact, a typical mode of locating the Na or Li resonance lines within the lab has become tuning the laser while listening for the sound wave produced when on resonance.

CROSLEY

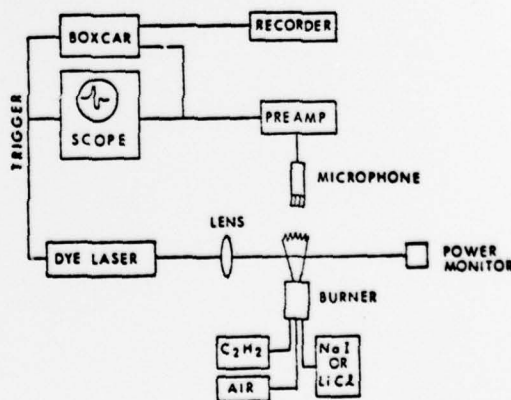
CHARACTERIZATION OF THE EFFECT

Experimental Details

The overall experimental arrangement is depicted in Fig. 1. The flame utilized in the experiments is an approximately stoichiometric mixture of C_2H_2 and air, seeded with Na atoms. (However, the generation of opto-acoustic pulses has also been accomplished using Li in the C_2H_2 /air flame, and with Na in a CH_4 /air flame). This is burned on a standard burner used for atomic absorption analytical measurements, so that the Na may be introduced by aspirating NaI solution. The Na atom number density was typically of the order of 10^{10} - 10^{11} cm^{-3} , as determined from both absorption and absolute fluorescence intensity measurements. The primary reaction zone at 1 atm extends only a few mm above the burner surface. The experiments are carried out at heights ranging from 0.5 to 3 cm above the surface, that is, in the region of the secondary reaction zone containing partially combusted gases.

The laser used is a Chromatix CMX-4, a commercially available flashlamp pumped tunable dye laser having a pulse duration of 1 μ sec. Although the laser is capable of delivering 10 mJ/pulse in the region of the Na resonance lines, it was here operated typically at < 1 mJ/pulse. The bandwidth is nominally 3 cm^{-1} and can be narrowed to 0.16 cm^{-1} by insertion of an etalon. (In a separate experiment, not further described here, opto-acoustic pulses have also been observed with a N_2 -laser-pumped-dye laser. The 5 nsec pulse lengths available with this instrument offer useful versatility with the technique).

Fig. 1. Experimental arrangement. The laser scanner, and a spectrometer often used for fluorescence observations, are not shown.



CROSLEY

The laser is focused to a few mm beam diameter and directed into the flame at a spot ~ 2 cm above the burner surface. When the laser is tuned to either of the two components of the 3^2P-3^2S transition in Na, the energy released in the quenching of the resonantly excited $3P$ state produces a pressure wave which propagates outward from the region illuminated by the laser. This sound wave is detected by a condenser microphone located ~ 4 cm from the flame. After amplification, the microphone signal is fed to an oscilloscope and to a boxcar (gated) integrator, both of which are triggered by a pulse from a photodiode detecting the laser pulse itself. Fig. 2 is a recorder tracing of the amplitude of the pressure wave signal vs. laser frequency. The laser is operated here in its narrowed mode and automatically scanned over the wavelength region which includes both doublet components. (The spikes marked 'etalon reset' are artifacts of the scanning sequence.) It is clear that the pressure waves result from the resonant electronic excitation and not from some other mode of laser energy deposition within the flame gases.

Magnitude of the Effect

We here calculate the amplitude of the pressure wave, given a simple picture of its formation, and compare the result with a measured value. The reasonable agreement achieved lends confidence to the physical picture, and shows that the pressure wave should not perturb the flame to any noticeable degree.

We consider a particular (though typical) experiment in which the Na absorbs 0.22 mJ from a single laser pulse, as the beam transverses a 1 cm path through the flame with a beam diameter of 1.5 cm. Over 99% of this energy is quenched; we assume that it immediately (on the

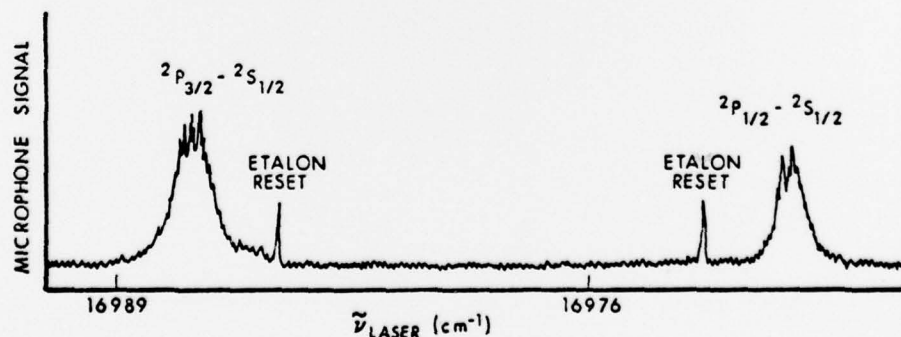


Fig. 2. Opto-acoustic pulse signal as a function of laser frequency.

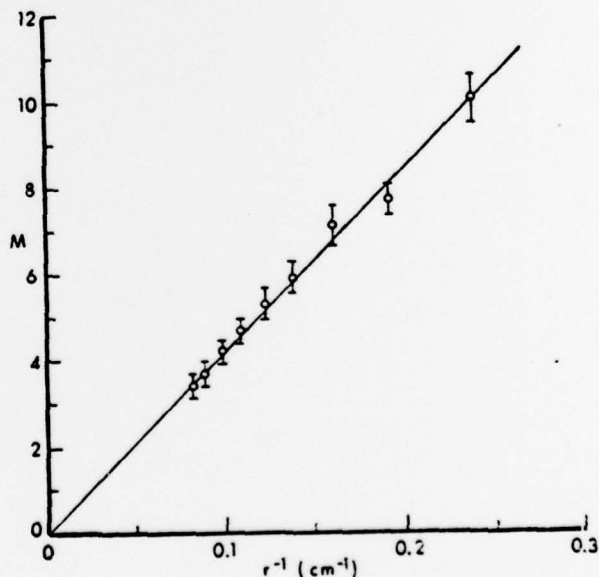
CROSLLEY

time scale of the laser pulse duration) is converted to translational energy* so that the illuminated region is effectively locally heated. This energy will then begin to spread into the surrounding regions of the flame. However, the laser pulse length, equivalent to a heating time, is shorter than the time it takes sound to traverse the heated region. Thus it is possible that a shock wave of very small amplitude is initially formed; if so, it soon degrades into a pulsed pressure wave.

The flame gases are assumed diatomic here, with a density appropriate to 1 atm and the flame temperature (from speed of sound measurements described below) of 2300°K. The irradiated volume of 1.75 cm³ thus has a heat capacity of 0.34 mJ/degree and is heated 0.64°K. This is a truly negligible amount of heating compared with the temperature of the flame gases themselves.

A pressure rise of 0.22 torr within the heated volume is calculated using the ideal gas law. This would produce an amplitude of 0.044 torr at the position of the microphone. (The expected inverse dependence on distance is verified by experiment; see Fig. 3.) The actual measured value** is 0.13 torr. In view of some contributions

Fig. 3. Dependence of pressure wave amplitude on flame-to-microphone distance r .



* See below for further comment on this process.

**Using a calibrated microphone.

CROSLEY

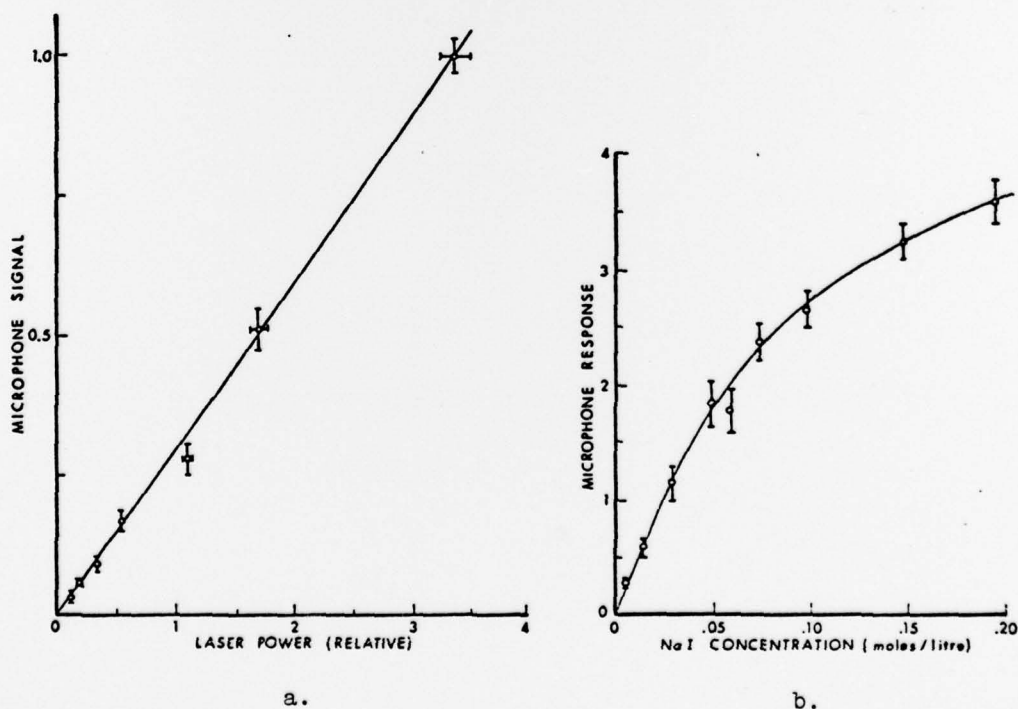
due to non-uniform irradiation, and especially the lack of knowledge concerning the actual mode of formation of the pressure wave, we consider this to be reasonable agreement.

This model suggests that the amplitude of the effect should be proportional to both the laser energy and the Na concentration. Fig. 4 shows such dependency. (In Fig. 4a, the laser power is well below the values later used for optically saturating the transition.) The high values of Na concentration in Fig. 4b exhibit non-linearity due to the large amount of absorption occurring.

Form of the Pressure Wave

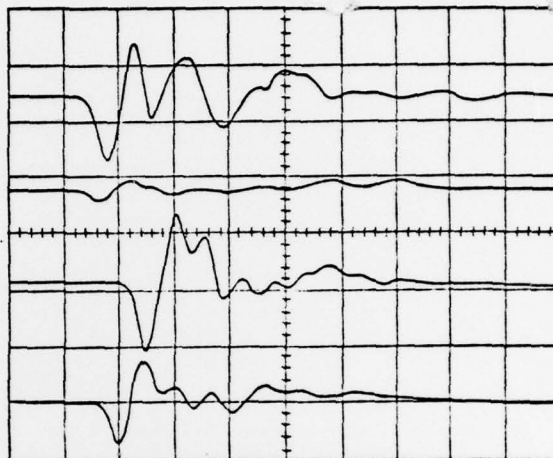
The form of the pressure wave is quite complex, and has been extensively examined although no quantitative information could be extracted. It is quite reproducible on a pulse to pulse basis for a fixed laser beam/flame/microphone geometry, though it varies as that

Fig. 4. a) Opto-acoustic signal as a function of laser power
b) opto-acoustic signal as a function of sodium concentration



CROSLEY

Fig. 5. Oscilloscope traces of opto-acoustic signal waveform, for 4 different geometrical arrangements. Each results from a single laser pulse. Horizontal axis: 20 μ sec per major division.



geometry is changed. Fig. 5 shows four oscilloscope traces for four different geometrical arrangements. The scope is triggered on the left by the photodiode, and the time scale here is 20 μ sec/cm. (The amplitude referred to throughout this paper is measured by setting the two boxcar gates to sample the first positive and negative extrema of the waveforms, and taking the difference.) The characteristics of the waveform, especially the smaller-amplitude oscillations following the first large wave, can be readily varied by introducing disturbances, particularly turbulence, into the flame. This implies that the form is dictated by reflections and/or interference from density gradients within the flame, though no analysis was attempted.

A sound wave having a frequency of the order of the inverse of some relaxation time (e.g., a vibrational energy transfer rate) within the system will undergo attenuation and phase shifts due to that relaxation process. Since vibrational relaxation times at 1 atm are of the order of the laser pulse duration, and since the laser pulse contains a spectrum of frequencies, it was hoped that a Fourier analysis of the waveform might yield information on these relaxation times within the flame. This approach was not successful, due to the dominance of the density gradient effects and the bandwidth (140 kHz) of our fastest microphone. "Air" mixtures of N_2/O_2 , Ar/O_2 , and CO_2/O_2 were tried in this series of experiments, but no differences could be discerned. With a faster microphone it remains possible that this will be a useful application of this technique.

CROSLEY

Even though the vibrational relaxation could not be directly observed in this manner, it is safe to conclude that the energy is transferred through the internal levels of the flame gases. N_2 , which constitutes some 60% of the total gas flow, has long been known to have a very high quench rate for electronically excited alkalis, especially Na. The suspicion that such high efficiency is due to the internal levels of the N_2 accepting the Na electronic energy has recently been borne out in a detailed experiment investigating the process.(6)

QUENCH RATE MEASUREMENTS

Descriptive Equations

Under conditions of high laser intensity, one may create an appreciable population in the electronically excited state. This will be the case when the rate, per atom, for absorption of laser light becomes comparable to the rate at which the atoms exit the upper state. Then, the number of excited atoms is no longer linear in the laser intensity. For Na, it is relatively easy to attain the necessary laser power density by focussing the beam, even for the high quench rates found in flames. This phenomenon is here used to measure the quenching rate of the excited state, which is the dominant term in determining its lifetime.

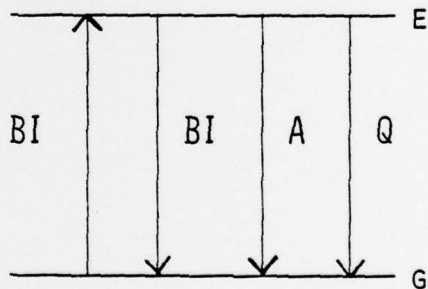


Fig. 6. Schematic illustration of 2-level system near optical saturation.

We consider a two-level system (see Fig. 6) and write a steady-state equation for the excited state number density N_e .

$$\frac{dN_e}{dt} = 0 = BIN_g - (BI + Q + A)N_e \quad (1)$$

The assumption of a steady state is valid since the time scales involved for the absorption and quenching processes are significantly shorter than the laser pulse duration. Here, B and A are the Einstein

CROSLEY

coefficients for absorption and spontaneous emission, respectively; the term BIN_e accounts for stimulated emission. I is the laser spectral power density, measured in (erg/sec) per cm^2 per unit frequency interval. Q is the total quench rate, per sec, for the upper level.

Since the total Na number density is a constant N_0 , i.e.

$$N_e + N_g = N_0,$$

Eq. (1) may be solved for the steady-state value of N_e

$$(N_e)_{s.s.} = \frac{BIN_0}{Q+A+2BI} \quad (2)$$

Now the opto-acoustic pulse signal M is proportional to $(N_e)_{s.s.}$:

$$M = c(N_e)_{s.s.},$$

where the constant represents the efficiency of conversion of electronic to translational energy, the microphone and amplifier characteristics and geometrical considerations. Substituting into Eq. (2), one has for the inverse of the microphone signal

$$M^{-1} = c' \left[2 + \left(\frac{Q+A}{B} \right) \frac{1}{I} \right] \quad (3)$$

Thus a plot of M^{-1} (in arbitrary units) vs. I^{-1} (in absolute units) should yield a straight line with a slope to intercept ratio of

$$\frac{Q+A}{2B} = \frac{Q/A+1}{2B/A}.$$

The relationship between B and A is known from thermodynamic considerations:

$$B = \frac{\lambda^3}{2hc} A,$$

so that the experimental result serves to determine Q/A . But if A has been separately measured, then an absolute value of Q may be extracted.

Experimental Results

Measurements were made at several heights above the burner surface. At each position, the microphone signal was measured as a function of laser intensity by inserting a series of neutral density filters into the laser beam. The data were taken in a manner alternating reference measurements with no filter and the signals with each given filter, in order to compensate for any drift in the overall laser power. The power measurements are made on an average power basis and reduced to instantaneous spectral power density

CROSLEY

($\text{erg cm}^{-2} \text{ sec}^{-1} \text{ Hz}^{-1}$) using the laser bandwidth, an assumed Gaussian gain profile, and observations of the pulse duration.

Fig. 7 shows a plot of the data for one run, in the form of Eq. (3). The error bars represent estimates of the readability of the box-car signals; the line is an unweighted least squares fit to the data. In this instance we obtain $Q/A \approx 410 \pm 40$. Using the value⁽⁷⁾ $A = 6.3 \times 10^6 \text{ sec}^{-1}$, this results in a $Q = (2.6 \pm 0.3) \times 10^{10} \text{ sec}^{-1}$.

The results for several heights above the burner are shown in Fig. 8. There is a marked falloff with height. This is at first surprising. Since the pressure across this flame is nearly constant, and the temperature decreases over this region, the number density is increasing with height. In addition, quenching rates should show little temperature dependence due to the exoergicity of the process. (In fact, the scanty data that does exist shows⁽⁸⁾ the $\text{N}_2\text{-Na}^*$ cross section dropping slightly in this temperature range.) This means that the observed variation of Fig. 8 must be caused by the presence of some species which itself has a large concentration gradient through this region. On the other hand, N_2 constitutes most of the flame gases. This molecule already has a large cross-section, so the species responsible must have a very large quench rate indeed. It is possible that the decrease reflects contributions from reactive quenching, an interpretation in accord with recent results of Schofield and Steinberg⁽⁹⁾ who find that in some flames, the overall Na concentration

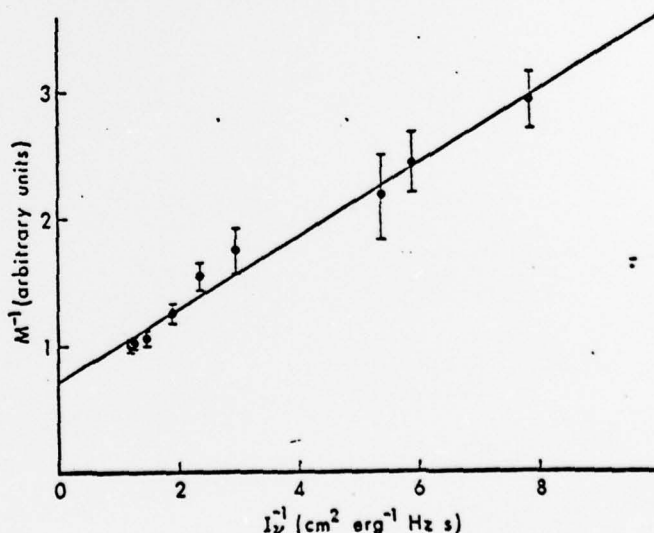
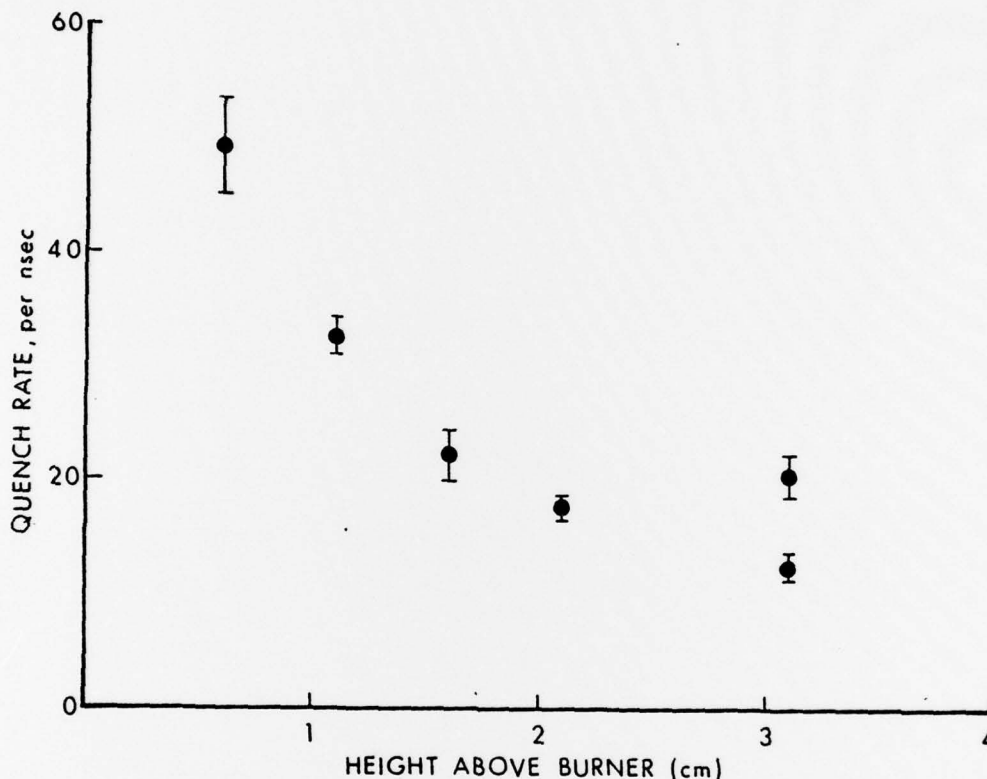


Fig. 7. Plot of inverse of microphone signal vs. inverse of laser spectral power density for quench rate determination.

CROSLEY

Fig. 8. Quench rate for Na 3^2P level as a function of height above the burner in a 1 atm acetylene-air flame.



drops with height due to NaOH formation. Also, the measured quench rates (10 to 50 per nsec) are substantially higher than the value (3 per nsec) calculated using the measured(10) bimolecular quench rates in a CH_4-O_2 flame and an assumed stoichiometric composition(11) for the current flame. This further suggests the presence of some intermediate species removing the Na($3P$) state by some means, reactive or non-reactive.

It should be noted that of course the $3P$ level of Na is a doublet, so that the simplified two-level scheme outlined above is inadequate. Since only one component of the doublet is pumped in any given experiment, collisional transfer rates between the two components enter into the steady-state expressions. The necessary accounting for such transfer can be performed only by making measurements

CROSLEY

on dispersed fluorescence following initial pumping of one level by the laser. Preliminary results(2) from such experiments indicate that the quench rates shown in Fig. 8 are uniformly higher than actual by about 11%. This of course would not change any of the inferences about the cause of the variation of Q with height.

For this series of measurements, the opto-acoustic pulses have served simply as a sensitive detector, and the fluorescence itself could have been used. However, the acoustic signal suffers from no reabsorption problems as does fluorescence, facilitating comparisons within different regions of the flame. This can be in general (and here is, in particular) an important advantage.

SPEED OF SOUND MEASUREMENTS

Both the oscilloscope and the boxcar are triggered by a pulse from a photodiode which responds to the laser firing. This enables the arrival time of the leading edge of the pressure pulse to be accurately measured. If the laser beam is then moved toward or away from the microphone, remaining in the flame and at the same height, the difference in arrival times together with the distance moved furnishes the speed of sound within the flame. (Although these measurements were made physically moving the beam for successive shots, a better method would be to split the beam into two or three components and obtain the information from one laser pulse, thus adding time resolution).

The measurements were made at three different heights well into the region of partially burned gases. The results were all the same, $(9.7 \pm 0.5) \times 10^4$ cm sec⁻¹, within experimental error. The uncertainty could be reduced by a more careful measurement of distances than was done for this demonstration experiment.

For a gas of average molecular weight \bar{M} and average heat capacity ratio $\bar{\gamma}$, the speed of sound u_s is related to the translational temperature by

$$u_s = [\bar{\gamma}RT/\bar{M}]^{1/2}$$

Again, a stoichiometric composition is used to calculate \bar{M} and $\bar{\gamma}$; the results are insensitive to this choice. The measured u_s corresponds to a temperature of $2280 \pm 230^\circ\text{K}$. For comparison, the adiabatic flame temperature for a stoichiometric acetylene air flame is 2545°K .(11)

The translational temperature is a most important flame characteristic, from the standpoint of both the gas dynamics and the

CROSLEY

chemical kinetics. The opto-acoustic pulse method offers the possibility of measuring the closely related speed of sound on a basis of high spatial and temporal resolution. No perturbation such as a thermocouple need be introduced into the flame, and extremely high temperatures (which are hostile to non-optical probes) appear to pose no fundamental difficulties. Such speed of sound measurements could well form the unique contribution of this method as a combustion diagnostic tool.

CONCLUSIONS

The experiments described here demonstrate that the pulsed opto-acoustic effect in a flame forms a sensitive and reproducible detector of the absorption of laser radiation by individual species within the flame. On the basis of the data such as that shown in Fig. 4, the magnitude of the observed effect can be scaled to very low values of overall absorption. Using the CMX4 laser, and this C_2H_2 /air flame, Na should be detectable at concentrations of $< 10^7$ atoms/cm³ with usable signal to noise; this is a partial concentration of < 0.01 ppb.

The method should be suitable for other species as well, as long as the overall quench mechanism is similar to the $E \rightarrow V \rightarrow T$ process here. It should be especially useful at high pressures where little of the absorbed laser energy appears as fluorescence but rather the excited state is predominantly quenched. For molecular systems, it holds promise for the detection of species which absorb but do not fluoresce at all, for example, due to rapid intersystem crossing (singlet to triplet) followed by quenching.

In addition, the method affords the ability to measure, rapidly and with spatial resolution, the speed of sound in a combusting mixture. The form of the pressure pulse produced, if it yields to analysis, holds information on density gradients within the flame and perhaps on relaxation phenomena within the flame gases.

ACKNOWLEDGMENTS

This project owes its success to the participation of, and contributions by, Drs. John E. Allen, Jr., and William R. Anderson, both NAS-NRC Postdoctoral Research Associates. The author gratefully acknowledges a pleasant and fruitful collaboration.

CROSLEY

REFERENCES

- (1) See, e.g., A. C. Eckbreth, P. A. Bonczyk and J. F. Verdick, United Technologies Research Center Report R77-952665-6, Hartford, Conn. (1977).
- (2) J. E. Allen, Jr., W. R. Anderson, D. R. Crosley and T. D. Fansler, 17th Symposium (International) on Combustion, Leeds, England, Aug. 1978.
- (3) D. Hartley, M. Lapp and D. Hardesty, Physics Today, Dec. 1975, p. 37.
- (4) R. B. Green, R. A. Keller, P. K. Schenck, J. C. Travis and C. G. Luther, J. Amer. Chem. Soc. 98, 8517 (1976).
- (5) A preliminary account is given in J. E. Allen, Jr., W. R. Anderson and D. R. Crosley, Optics Letters 1, 118 (1977).
- (6) I. V. Hertel, H. Hofmann and K. A. Rost, Phys. Rev. Lett. 36, 861 (1976); Chem. Phys. Lett. 47, 163 (1977).
- (7) A compilation of Na lifetime measurements is contained in N. Ioli, F. Strumia and A. Moretti, J. Opt. Soc. Am. 61, 1251 (1971).
- (8) P. L. Lijnse and R. J. Elsenaar, J. Quant. Spectr. Radiat. Trans. 12, 1115 (1972).
- (9) M. Steinberg, Univ. Calif. at Santa Barbara, private communication, Feb. 1978.
- (10) H. P. Hooymayers and C. Th. J. Alkemade, J. Quant. Spectr. Radiat. Trans. 6, 847 (1966).
- (11) A. G. Gaydon and H. G. Wolfhard, Flames, 3rd Ed., (Chapman and Hall, London 1970).